



**HAL**  
open science

## **A chronology of Holocene and Little Ice Age glacier culminations of the Steingletscher, Central Alps, Switzerland, based on high-sensitivity beryllium-10 moraine dating**

Irene Schimmelpfennig, Joerg M. Schaefer, Naki Akçar, Tobias Koffman, Susan Ivy-Ochs, Roseanne Schwartz, Robert C. Finkel, Susan Zimmerman, Christian Schlüchter

► **To cite this version:**

Irene Schimmelpfennig, Joerg M. Schaefer, Naki Akçar, Tobias Koffman, Susan Ivy-Ochs, et al.. A chronology of Holocene and Little Ice Age glacier culminations of the Steingletscher, Central Alps, Switzerland, based on high-sensitivity beryllium-10 moraine dating. *Earth and Planetary Science Letters*, 2014, 393, pp.220 - 230. 10.1016/j.epsl.2014.02.046 . hal-01682738

**HAL Id: hal-01682738**

**<https://hal.science/hal-01682738>**

Submitted on 8 Feb 2019

**HAL** is a multi-disciplinary open access archive for the deposit and dissemination of scientific research documents, whether they are published or not. The documents may come from teaching and research institutions in France or abroad, or from public or private research centers.

L'archive ouverte pluridisciplinaire **HAL**, est destinée au dépôt et à la diffusion de documents scientifiques de niveau recherche, publiés ou non, émanant des établissements d'enseignement et de recherche français ou étrangers, des laboratoires publics ou privés.

1 **A chronology of Holocene and Little Ice Age glacier culminations of the Steingletscher, Central**  
2 **Alps, Switzerland, based on high-sensitivity beryllium-10 moraine dating**

3

4 Irene Schimmelpfennig<sup>a,b\*</sup>, Joerg M. Schaefer<sup>a</sup>, Naki Akçar<sup>c</sup>, Tobias Koffman<sup>a,d</sup>, Susan Ivy-Ochs<sup>e</sup>,  
5 Roseanne Schwartz<sup>a</sup>, Robert C. Finkel<sup>f,g</sup>, Susan Zimmerman<sup>f</sup>, Christian Schlüchter<sup>c</sup>

6 <sup>a</sup>*Lamont-Doherty Earth Observatory, Columbia University, Palisades, New York 10964, USA*

7 <sup>b</sup>*Aix-Marseille Université, CNRS-IRD-Collège de France, UM 34 CEREGE, Aix-en-Provence, France*

8 <sup>c</sup>*Institute of Geological Sciences, University of Bern, Switzerland*

9 <sup>d</sup>*Department of Earth Sciences and Climate Change Institute, University of Maine, Orono, ME 04469, USA*

10 <sup>e</sup>*Institut für Teilchenphysik, Eidgenössische Technische Hochschule, Zürich, Switzerland*

11 <sup>f</sup>*Center for Accelerator Mass Spectrometry, Lawrence Livermore National Laboratory, Livermore, CA 94550, USA*

12 <sup>g</sup>*Earth and Planetary Science Department, University of California–Berkeley, Berkeley, California 94720, USA*

13

14 \*corresponding author:

15 E-mail: [schimmel@cerege.fr](mailto:schimmel@cerege.fr)

16 Phone: +33 442971556

17 Present address: CEREGE, Europôle de l'Arbois, 13454 Aix en Provence Cedex 4, France

18

19 Abbreviations:

20 CE: Common Era; ELA: equilibrium line altitude; KDE: Kernel Density Estimation; LIA: Little Ice  
21 Age; PAM: Partitioning Around Medoids; PDP: Probability Density Plot; YD: Younger Dryas

22

## 22 **ABSTRACT**

23 The amplitude and timing of past glacier culminations are sensitive recorders of key climate events on  
24 a regional scale. Precisely dating young moraines using cosmogenic nuclides to investigate Holocene  
25 glacier chronologies has proven challenging, but progress in the high-sensitivity  $^{10}\text{Be}$  technique has  
26 recently been shown to enable the precise dating of moraines as young as a few hundred years. In this  
27 study we use  $^{10}\text{Be}$  moraine dating to reconstruct culminations of the Steingletscher, a small mountain  
28 glacier in the central Swiss Alps, throughout the Holocene. The outermost-recorded positions of  
29 Steingletscher most likely occurred in the Early Holocene and appear nearly synchronous with glacier  
30 culminations reported from other regions in the Alps. A Late-Holocene position corroborates the  
31 evidence for a significant glacier advance of similar extent to that of the Little Ice Age (LIA)  $\sim 3$  kyr  
32 ago. Finally, fourteen boulders from different moraines yield  $^{10}\text{Be}$  ages between 580 and 140 years  
33 with analytical precisions mostly  $< 10\%$ , dating Steingletscher advances during the LIA. Because these  
34 LIA  $^{10}\text{Be}$  ages are in stratigraphic order, we tentatively distinguish four LIA glacier culminations:  
35 about 1470 CE, 1650 CE, 1750 CE and 1820 CE, which are in good agreement with existing  
36 independent records during the LIA in the Swiss Alps. These findings illustrate the high potential of  
37 the  $^{10}\text{Be}$  moraine dating method to directly link paleo-glacier-chronologies to historical records and  
38 thus present-day glacier evolution.

39

40 *Keywords: Glacier fluctuations; Holocene; Little Ice Age;  $^{10}\text{Be}$  moraine dating; Swiss Alps; climate*  
41 *change*

42

## 43 **1. Introduction**

44 Glaciers are sensitive recorders of regional climate variations (e.g. Oerlemans, 2005). Therefore, the  
45 investigation of glacier behavior in the past represents a powerful means to reconstruct terrestrial  
46 paleoclimate variability. In particular, understanding the response of glaciers to climate variability  
47 during the Holocene, the current interglacial which started ~11,700 years ago (Rasmussen et al., 2007),  
48 offers the opportunity to assess the effects of ongoing climate change, because climate conditions were  
49 similar to those existing at the present. The Holocene is characterized by moderate-amplitude climate  
50 change resulting in glacier extents in the Northern Hemisphere that were larger as well as smaller than  
51 today (e.g. Joerin et al. 2006; Ivy-Ochs et al., 2009 and references herein). Historical records of glacier  
52 advances during the Little Ice Age (LIA, 14<sup>th</sup> to 19<sup>th</sup> century; Grove, 2001; Holzhauser et al., 2005)  
53 and the subsequent rapid glacier retreats provide clear evidence for significant centennial climate  
54 variability in the recent past. In the Alps, detailed chronologies of the two largest Swiss glaciers, Great  
55 Aletsch and Gorner, inferred from radiocarbon-dating, dendrochronology, archeology and historical  
56 data, imply three major glacier advances during the LIA: around 1300-1380 CE, 1600-1670 CE and  
57 1800-1860 CE (Holzhauser et al., 2005). Evidence from the smaller Lower Grindelwald glacier  
58 indicates similar peaks with additional variability (Holzhauser et al., 2005). Existing chronological  
59 documentation of Holocene glacier fluctuations in the Alps pre-dating the LIA is mostly based on  
60 radiocarbon-dated subfossil wood, peat, soil, and archeological finds from glacier forefields (e.g.  
61 Roethlisberger and Schneebeli, 1979; Baroni and Orombelli, 1996; Hormes et al., 2001; review in Ivy-  
62 Ochs et al., 2009). In addition, some pioneering data has been produced during recent years from  
63 surface exposure dating of glacio-geomorphic features, in particular moraines (Ivy-Ochs et al., 1996,  
64 2006; Kelly et al., 2004; Goehring et al., 2011a; Schindelwig et al., 2012; Schimmelpfennig et al.,  
65 2012; Cossart et al., 2012).

66 Moraines constitute valuable geomorphic markers of past climate, because they mark glacier  
67 culminations, i.e. periods when a glacier began to retreat from an advanced position. Dating the  
68 deposition of moraines using cosmogenic nuclides therefore allows the timing of past climate changes  
69 to be determined. However, Holocene moraine chronologies are scarce in the Alps, because the LIA  
70 advances destroyed the older moraines in many places (e.g. Röthlisberger and Schneebeli, 1979).  
71 While the few previous Holocene surface exposure dating studies in the Alps mostly focused on  
72 glacier positions during the Late Glacial/Early Holocene transition (Ivy-Ochs et al., 2009), recent  
73 works show that the high-sensitivity cosmogenic  $^{10}\text{Be}$  method also affords the dating of moraines as  
74 young as the LIA (e.g. Schaefer et al., 2009; Licciardi et al., 2009; Schimmelpfennig et al., 2012;  
75 Akçar et al., 2012).

76 At Steingletscher (“Stein glacier”), in the Central Swiss Alps, particularly well-resolved moraines and  
77 moraine remnants are preserved on and beyond the visible LIA extent of the glacier (Fig. 1). The  
78 glacier forefield of Steingletscher was previously the object of a thorough glaciological and  
79 paleoclimatic study by King (1974), which includes a moraine map as well as palynological  
80 investigations and bracketing radiocarbon dates from peat bog profiles and fossil soils related to the  
81 moraine deposits (Fig. 1).

82 In this study, we measured a detailed chronology of the Steingletscher moraine sequence based on  
83 cosmogenic  $^{10}\text{Be}$  with the overall goal of reconstructing the glacier culminations recorded by these  
84 moraines throughout the Holocene. By comparing our results with previous studies, we focus on two  
85 particular questions: (1) Were Early-Holocene glacier culminations synchronous, time-transgressive or  
86 unrelated throughout the Alps? (2) Can we resolve individual glacier peaks during the Late Holocene  
87 and the LIA using high-sensitivity  $^{10}\text{Be}$  surface exposure dating? By tackling this second question, we

88 aim to test a dating method complementary to radiocarbon dating to investigate the timing and fine  
89 structure of regional climate variations in the Alps on this recent time-scale.

90

## 91 **2. Study site and geomorphic setting**

92 Steingletscher (~47°N, 8°W) is a small mountain glacier (length ~4 km, surface area ~6 km<sup>2</sup>;  
93 Glaciological reports, 1881-2009), located in the easternmost part of the Canton Berne, west of the  
94 Susten pass in the Central Alps. The surrounding geology comprises highly metamorphosed pre-  
95 Mesozoic metagranitoids, gneisses and amphibolites. In Meiringen, the closest weather station (589 m  
96 above sea level), the monthly mean temperatures between 1981 and 2010 CE ranged from -1.4°  
97 (January) to 17.7°C (July); annual mean precipitation was 1375 mm; and snow cover occurred on  
98 average 71 days per year.

99 Proglacial lake Steinsee (Figs. 1, 2A and C) developed in front of the main Steingletscher tongue in  
100 1924 CE (Blass et al., 2003). This lake and four minor glaciers at the head of the catchment drain into  
101 the Gadmen Valley, a westward trending tributary of the Aare Valley.

102 The following description of the most striking and datable moraines and glacial boulders and their  
103 illustration in the left panel of Fig. 1 are based on field observations and interpretation of Google Earth  
104 images. They are not based on King's (1974) earlier moraine map (Fig. 1C).

105 On the left-lateral side near the catchment's outlet, two groups of roughly parallel moraine ridges and  
106 relicts are preserved on 'Hublen', a roche moutonnée plateau at 2060 m elevation. The two moraine  
107 groups are about 60 m laterally apart (Fig. 1) and ~60 m and 70 m higher, respectively, than the LIA  
108 limit visible on the eastern flank of the plateau. In the following we will refer to these moraines as the  
109 'outer moraine' and the 'inner moraine relicts' on the Hublen plateau. Few boulders exist on the crests  
110 or slopes of these ridges (Fig. 2C). To the north, 200 m lower at the eastern end of the 'In Miseren'

111 plateau, another moraine ridge is preserved, oriented obliquely to the close-by valley bottom at an  
112 angle of about 40° (Fig. 1). This moraine is located ~150 m outside of the visible LIA limit. Several  
113 big boulders are embedded in its crest. While the geometry of this lower moraine suggests the presence  
114 of a glacier terminus lying only a few hundred meters downstream of the catchment's outlet, no  
115 geomorphic hints for such a terminal moraines corresponding to the upper moraines on the Hublen  
116 plateau could be found. According to King (1974), the two moraine groups on the Hublen plateau and  
117 the one on the In Miseren plateau actually represent the glacier at three very different stages. King  
118 (1974) assumes that the two moraine groups on the Hublen plateau were deposited during the  
119 regionally defined Late Glacial stadials 'Daun' and 'Egesen', respectively (in Ivy-Ochs et al., 2006 and  
120 references therein). These culminations are chronologically related to a cold interval preceding the  
121 Bølling warm interval ~15 kyr ago and to the Younger Dryas 12.9-11.7 kyr ago, respectively, with  
122 equilibrium line altitudes of a few hundred meters below that of the LIA (Ivy-Ochs et al., 2006 and  
123 references therein). King (1974) therefore suggests that the terminal positions corresponding to the  
124 outer and inner moraines on the Hublen plateau might have been ~6 km (near the Gadmén village) and  
125 ~3 km (in the area of the Wysemaad creek) down the valley, respectively. King assigns the moraine  
126 on the In Miseren plateau to the Holocene (Fig. 1C).

127 About 180 m further downstream of the moraine on the In Miseren plateau, three huge boulders  
128 protrude from a sediment mound close to the valley bottom. While King (1974) presumably mapped  
129 this deposit as part of a moraine (Fig. 1C), a rockfall-related origin cannot entirely be excluded. In  
130 addition, it is unclear if the deposit has at anytime in the past been affected by washout from the glacial  
131 stream. Therefore, we conservatively represent it as boulders on a glaciofluvial deposit in Fig. 1.

132 The LIA extent of Steingletscher is well marked by a vegetation change (trimline) in the glacier  
133 forefield nearly encircling the lake at a distance of up to 400 m (Figs. 2A and C). The trimline serves

134 as a morphostratigraphic reference marker for glacier advances relative to the LIA positions. Moraines  
135 on this limit are preserved at various locations, i.e. on the right-lateral side east of the lake (massive  
136 composite moraine, Fig. 2C) as well as next to the catchment's outlet (moraine segments), and on the  
137 left-lateral side on the glacier-proximal hill Chüebergli (sharp ridge, Figs. 1, 2B) and in the  
138 prolongation of the northern flank of the Bockberg mountain (sequence of interlaced and blocky ridges,  
139 Fig. 1, Fig. 2E). At all locations on the LIA limit, except the composite moraine, several individual  
140 sub-ridges can be distinguished. Inboard of the LIA-limit, historical moraines correspond to the years  
141 1920 CE (King, 1974) and 1988 CE (Figs. 1, 2D, 3).  
142 The profile and outcrop locations investigated and dated by King (1974) are depicted in Fig. 1. His  
143 calibrated radiocarbon ages are shown in Fig. 1, 4G and in Table 2.

144

### 145 **3. Methodology**

146 We targeted 30 large granitic boulders, embedded in the crests or slopes of moraines, for the well-  
147 established  $^{10}\text{Be}$  moraine dating method (e.g. Schaefer et al., 2009; sample locations in Fig 1; sample  
148 details in Table 1). On moraines with only few boulders, we sampled all boulders that matched these  
149 criteria, whereas from blockier moraines, we chose several of the most suitable boulders, making an  
150 effort to sample various sub-ridges where possible, notably on the LIA limit. The boulders are gneiss,  
151 some with quartz veins, which we preferentially targeted for sampling. Using hammer and chisel, we  
152 collected samples with thicknesses of 1-5 cm from the center of flat-topped surfaces of these boulders.  
153 All samples were processed at the Lamont-Doherty Earth Observatory Cosmogenic Nuclide  
154 Laboratory (method in Schaefer et al., 2009), where the quartz was chemically isolated by leaching the  
155 crushed and sieved bulk rock, first in boiling orthophosphoric acid and then in dilute  
156 hydrofluoric/nitric acid. Purified quartz yields ranged between 7 g and 72 g (Table 1). Usually,

157 younger samples require greater quartz weights than older samples. Taking advantage of improvement  
158 in detection limits for  $^{10}\text{Be}$ , we tested in this study the possibility of using as little as 7 g quartz for  
159 some of the youngest boulders in the data set, which was the maximum quartz weight we could isolate  
160 from these samples. As discussed in detail in the next section, the numbers of atoms  $^{10}\text{Be}$  in these small  
161 samples are one to two orders of magnitude higher than the blanks, implying that at certain study sites  
162 using less than 10 g quartz can be sufficient to date boulders that have been exposed for only a few  
163 hundred years, if laboratory and measurement detection limits are sufficiently low. The ability to use  
164 small samples greatly simplifies the chemical isolation of  $^{10}\text{Be}$ . The extraction of  $^{10}\text{Be}$  from the  
165 purified quartz is described in detailed at <http://www.ldeo.columbia.edu/tcn/>.  $^{10}\text{Be}/^9\text{Be}$  ratios were  
166 measured at the Center for Accelerator Mass Spectrometry of the Lawrence Livermore National  
167 Laboratory. To derive the surface exposure ages from the determined  $^{10}\text{Be}$  concentrations, we used the  
168 calculation methods incorporated in the CRONUS-Earth online exposure age calculator (Balco et al.,  
169 2008). We applied the “Arctic”  $^{10}\text{Be}$  production rate recently established by Young et al. (2013), which  
170 includes previously and newly produced Holocene calibration data sets from Northern Hemisphere  
171 sites at latitudes  $>40^\circ$ , in combination with the time-dependent version of the scaling model by Lal  
172 (1991). This production rate has a reference value of  $3.96 \pm 0.15$  atoms  $^{10}\text{Be} \text{ g}^{-1} \text{ yr}^{-1}$  at sea level and  
173 high latitude. Other recently published production rates are up to  $\sim 5\%$  lower (e.g. Putnam et al., 2010;  
174 Fenton et al., 2011) and  $\sim 3\%$  higher (Goehring et al., 2011b), and would in our study yield ages that  
175 are correspondingly higher and lower, respectively.

176 The uncertainties in the ages given in the text below include the error in the Arctic production rate  
177 unless otherwise mentioned. All ages are referenced to the year 2010 CE.

178 In our age calculations we did not include corrections for boulder surface erosion because of the high  
179 resistance of the sampled lithologies to weathering and the lack of any signs of significant erosion on

180 the sampled surfaces. Assuming an erosion rate of  $1 \text{ mm kyr}^{-1}$ , an upper bound postglacial weathering  
181 rate for crystalline rocks (André, 2002), would increase the ages by  $< 1\%$ , which would not affect our  
182 conclusions.

183 We did not correct our  $^{10}\text{Be}$  ages for any potential snow cover, because quantitative records of snow  
184 thickness and duration do not exist for the time-periods considered here. We deem considerable snow-  
185 effects unlikely, because boulders protruding from the moraine crests are often exposed to strong  
186 winds at these altitudes, minimizing the likelihood that snow remained on the sampled surfaces for  
187 significant time. Assuming the improbable scenario of a continuous snow cover of 30 cm for 4 months  
188 would result in an increase of the exposure ages by  $< 2\%$ , which would not impact our conclusions.

189

#### 190 **4. Results**

191 The resulting boulder exposure ages are shown in Fig. 1 and in Table 1. As detailed in the following,  
192 all ages are in agreement with their stratigraphic position, i.e. younger ages correspond to more glacier-  
193 proximal positions.

194 Two boulders slightly inboard of the outer moraine crest on the Hublen plateau yield ages of  $10,860 \pm$   
195  $460 \text{ yr}$  and  $10,580 \pm 450 \text{ yr}$  (arithmetic mean:  $10,720 \pm 440 \text{ yr}$ ). The ages of three boulders sampled  
196 from the close-by inner moraine relicts on the same plateau are  $10,490 \pm 480 \text{ yr}$ ,  $10,320 \pm 490 \text{ yr}$  and  
197  $10,030 \pm 450 \text{ yr}$ . Three boulder ages on the crest of the 200 m lower left-lateral moraine are  $10,090 \pm$   
198  $410 \text{ yr}$ ,  $9400 \pm 370 \text{ yr}$ , and  $8350 \pm 330 \text{ yr}$ , being less consistent than those of all other moraines at  
199 Steingletscher. We regard the age of  $8350 \pm 330 \text{ yr}$  as an outlier, based on the observation that glaciers  
200 in the Swiss Alps appear to have been smaller than today for about a thousand years before  $\sim 8.2 \text{ kyr}$   
201 ago, when they briefly re-advanced to a position similar to the present-day extent (Joerin et al., 2006;  
202 Nicolussi and Schlüchter, 2012). The arithmetic mean of the two older boulder ages is  $9,740 \pm 610 \text{ yr}$ .

203 One boulder slightly inboard of this moraine ridge yields an age of  $2,850 \pm 130$  yr, and another boulder  
204 on the right-lateral side, located slightly outboard of the 'LIA limit' gives an age of  $2,870 \pm 120$  yr.  
205 The three boulders on the glaciofluvial deposit near the bottom of the glacier valley yield similar and  
206 very consistent ages of  $2,830 \pm 120$  yr,  $2,720 \pm 120$  yr and  $2,710 \pm 130$  yr with an arithmetic mean age  
207 of  $2,750 \pm 130$ . Amongst 15 boulder ages on the LIA limit, fourteen range between  $580 \pm 50$  yr and  
208  $140 \pm 30$  yr, and one age from a huge boulder is  $1,816 \pm 77$  yr. We consider this significantly older  
209 boulder age as an outlier. Remarkably, at the locations on the LIA limit where individual sub-ridges  
210 are distinguishable, the ages between  $\sim 580$  yr and  $\sim 140$  yr are in stratigraphic order, i.e. the further  
211 inboard the moraine the younger the boulder age. For example, on the hill Chüebürgli boulders STEI-  
212 18 and STEI-15, which are located on the sharp outer crest, yield ages of  $\sim 310$  yr and  $\sim 280$  yr,  
213 respectively, whereas boulder STEI-17 from a close-by inner sub-ridge is dated to  $\sim 190$  yr (Figs. 1,  
214 2B). Similarly, at the moraine ridge sequence north of the Bockberg mountain, the oldest boulders  
215 STEI-12-23 and STEI-12-13 ( $\sim 580$  yr and  $\sim 530$  yr, respectively) are from the outmost position of the  
216 discernable moraine ridges, whereas the youngest boulder STEI-12-20 is from the innermost position  
217 of all boulders dated at this location (Fig. 1).

218 Inboard of the LIA limit, one boulder 15 m below the 1920 CE moraine (STEI-16) yields  $162 \pm 10$  yr,  
219 and one boulder from the 1988 CE moraine crest (STEI-7) yields  $127 \pm 8$  yr. The significance of these  
220 post-LIA boulders will be discussed below.

221 Concerning the amounts of quartz used to determine the 16 youngest boulder ages in our data set  
222 ( $< 600$  years), we note here that the  $1\sigma$  analytical uncertainties of the samples processed with quartz  
223 weights of 24 - 70 g range between 2% and 6%, and those processed with unusual low quartz weights  
224 of 7 - 20 g are between 6% and 13%, except sample STEI-12-20 with 24% (Table 1). The numbers of  
225 atoms  $^{10}\text{Be}$  of the low quartz weight samples range between  $32 \times 10^3$  and  $121 \times 10^3$  atoms, while

226 associated blanks are between  $3 \times 10^3$  and  $7 \times 10^3$  atoms, corresponding to blank corrections of 2% to  
227 13% (Table 1). Blank-corrected  $^{10}\text{Be}$  concentrations of these samples are between  $3 \times 10^3$  and  $12 \times 10^3$   
228 atoms  $^{10}\text{Be g}^{-1}$  quartz (Table 1). These results show that, if laboratory and measurement backgrounds  
229 allow for low detection limits, reliable  $^{10}\text{Be}$  measurements well above the blank level can be achieved  
230 even when using only 10-20 g or less quartz from moraine boulders that were deposited during the last  
231 few hundred years. This might be of interest for studies, in which limited precision is acceptable and  
232 elevations are similar to or above those in our study.

233

## 234 **5. Discussion**

235 Our Steingletscher moraine chronology (Fig. 1) implies temporal constraints for glacier culminations  
236 during the Early Holocene, the Late Holocene and the LIA, which we compare here with other  
237 Holocene glacier studies in the European Alps and oxygen isotope records in Greenland ice cores and  
238 in Swiss lake sediments (Fig. 4 and 5).

239

### 240 5.1 Early Holocene versus Late Glacial:

241 The  $^{10}\text{Be}$  exposure ages presented suggest that Early Holocene glacier extents at Steingletscher are  
242 recorded at two locations: (1) On the Hublen plateau, where the two parallel lateral moraine groups  
243 indicate an Early Holocene glacier extent significantly beyond the LIA glacier position. The outer  
244 moraine corresponds to a glacier culmination that is dated to at least  $\sim 10.7$  kyr ago. The actual  
245 culmination could have occurred somewhat earlier, as the two dated boulders are located slightly  
246 inboard of the moraine crest. The ages from inner moraine relicts on the Hublen plateau, decreasing  
247 from  $\sim 10.5$  kyr to  $\sim 10.0$  kyr, suggest a slow oscillatory retreat over a few hundred years. (2) On the  
248 200 m lower In Miseren plateau, the boulder ages from the preserved moraine ridge yield an only

249 slightly younger arithmetic mean age of ~9.7 kyr. This moraine, however, represents a much  
250 diminished glacier extent, close to that of the LIA. Therefore it appears to correspond to a significantly  
251 smaller glacier size than that represented by the moraines on the Hublen plateau, suggesting that the  
252 glacier underwent considerable melting within a few hundred years before ~9.7 kyr ago.

253 We note that the choice of the  $^{10}\text{Be}$  production rate for the age calculations (Section 3) introduces  
254 uncertainties in the calculated ages. Using the almost 5% lower production rate calibrated in New  
255 Zealand (Putnam et al., 2010) would yield an age for the oldest boulder in the data set whose  
256 uncertainties slightly overlap with the end of the last Late Glacial cold phase, the Younger Dryas (YD),  
257 ~11.7 kyr ago. Therefore, a deposition of the outer moraine during the late YD cannot entirely be  
258 excluded. However, according to the traditional picture in the Alps, equilibrium line altitudes during  
259 the YD (regionally referred to as the Egesen stadial, Section 2) were ~200-450 m below that of the LIA  
260 (Ivy-Ochs et al., 2006 and references therein). Since we consider such a large ELA depression unlikely  
261 for the outer moraine on the Hublen plateau, it appears more plausible that the outmost moraines of  
262 Steingletscher were deposited during the Early Holocene.

263 Our data suggest that King's (1974) assignment of the two moraine groups on the Hublen plateau to  
264 the Late Glacial stadials Daun and Egesen, respectively (Section 2), overestimates the ages of these  
265 moraines by a few thousand years. However, his minimum ages of 10710 – 10260 cal. yr before 2010  
266 CE (peat bog profile ST5) and 10290 – 8470 cal. yr before 2010 CE (peat bog profile ST1) for the  
267 moraines on the Hublen plateau and of 7850 – 7480 cal. yr before 2010 CE (peat bog profile ST9) for  
268 the moraine on the In Miseren plateau do fall into the Early and mid-Holocene and are in agreement  
269 with our results (Fig. 1; Fig. 4G, Table 2).

270 Early Holocene  $^{10}\text{Be}$  moraine ages have previously been suggested at several locations in the Alps, i.e.  
271 for the prominent left-lateral moraine of the Great Aletsch glacier (Kelly et al., 2004), the Kartell site

272 moraine (Ivy-Ochs et al., 2006), four moraines at the Belalp site (Schindelwig et al., 2012) and the  
273 outmost moraine of the Tsidjiore Nouve Glacier (Schimmelpfennig et al., 2012). In the original studies,  
274 ages were calculated with different  $^{10}\text{Be}$  production rates from the one we used here. We therefore  
275 recalculated these published ages using the Arctic production rate (Tables S1 in Supplement) and  
276 plotted for each moraine the summed probability curves of all boulder ages (excluding those  
277 considered outliers in the original studies) in Fig. 4 for comparison with the Steingletscher results. The  
278 Arctic  $^{10}\text{Be}$  production rate is lower than the production rates previously used in the studies of Kelly et  
279 al. (2004), Ivy-Ochs et al. (2006) and Schindelwig et al. (2012), therefore making these recalculated  
280 ages older than in the original publications by 10-20%. The moraine ages at Tsidjiore Nouve glacier  
281 become younger by 2.8%, because Schimmelpfennig et al. (2012) used the slightly lower  $^{10}\text{Be}$   
282 production rate calibrated by Balco et al. (2009) in Northeast North America.

283 In Fig. 4 the panels C-F and H show the recalculated moraine ages of all sites sorted as a function of  
284 their location from west to east in order to investigate the possibility of a potential time-transgressive  
285 trend of the glacier culminations along the Alps. The figures illustrate that the Early Holocene moraine  
286 ages of Steingletscher from the Hublen plateau (red and blue curves in Fig. 4F) agree within their  $1\sigma$   
287 uncertainties with those of the Tsidjiore Nouve Glacier and with the innermost Belalp moraine, while  
288 the broader age distribution of the moraine on the In Miseren plateau (green curves in Fig. 4F) only  
289 overlaps with the innermost Belalp moraine. No temporal trend can be detected based on these data. As  
290 has been suggested in the previous moraine chronology studies (Kelly et al., 2004; Ivy-Ochs et al.,  
291 2006, 2009; Schindelwig et al., 2012; Schimmelpfennig et al., 2012), these Early Holocene glacier  
292 culminations might be related to abrupt cold spells inferred from oxygen-isotope records in Greenland  
293 ice cores, such as the Preboreal Oscillation  $\sim 11.4$  kyr ago, the 10.9 kyr, and 9.3 kyr event (e.g.  
294 Rasmussen et al., 2007; Severinghaus et al., 2009; Fig. 4A). Independent paleoclimate studies support

295 the impact of short Greenland cold snaps in the Alps. In particular, the  $\delta^{18}\text{O}$  changes in Swiss lake  
296 sediments, which show a remarkable similarity with the Greenland  $\delta^{18}\text{O}$  record, include Early  
297 Holocene signals that strongly resemble the signatures of the PBO and possibly a part of the 10.9 kyr  
298 event in Greenland (Schwander et al., 2000; Fig. 4B). However, a clear assignment of the three mean  
299 ages from the Early Holocene moraines of Steingletscher to specific abrupt cold events needs further  
300 investigation to more tightly constrain the chronology of these glacio-geomorphic features.

301

### 302 5.2 Mid-Holocene:

303 At Steingletscher, no moraines are preserved from the mid-Holocene. This observation is in agreement  
304 with the Holocene moraine record observed at the Tsidjiore Nouve Glacier (Schimmelpfennig et al.,  
305 2012) and the findings at many other glaciers in the Alps (review in Ivy-Ochs et al., 2009). Due to the  
306 warm mid-Holocene climate, glaciers had retreated at least as far into their valleys as they are today, as  
307 evidenced by radiocarbon-dated subfossil wood and peat (Joerin et al., 2006, 2008). The subsequent  
308 glacier re-advances during the Late Holocene overran any moraines that might have formed during the  
309 Middle Holocene.

310

### 311 5.3 Late Holocene:

312 The strikingly similar Late-Holocene ages of the two single boulders on each side of the catchment's  
313 outlet (~2.9 kyr) and of the three huge boulders on the glaciofluvial deposit near the valley bottom  
314 (mean age ~2.8 kyr) (Fig. 1) suggest that their deposition was synchronous and related to the same  
315 glacier advance slightly outside of the LIA-limit. This supports the possibility that the three huge  
316 boulders in the valley center might be closely associated with a Late Holocene glacier terminal  
317 position. King (1974) also provides evidence for a glacier extent similar to that of the LIA around ~3

318 kyr ago at four different locations on the right-lateral side of the catchment's outlet at Steingletscher  
319 constrained by two minimum ages of 2520 – 2010 cal. yr before 2010 CE (profile Steinalp) and 3400 –  
320 2800 cal. yr before 2010 CE (profile Hotel 1) and two maximum ages of 3510 – 3020 cal. yr before  
321 2010 CE (profile Hotel 2) and 4020 – 3650 cal. yr before 2010 CE (outcrop Grabung D)(Figs. 1, 4G;  
322 Table 2). The evidence from our  $^{10}\text{Be}$  boulder ages and King's (1974) radiocarbon-dates at  
323 Steingletscher reinforces the Late Holocene finding from Tsidjiore Nouve Glacier in Schimmelpfennig  
324 et al. (2012) (cf. Fig. 4C) indicating that both glaciers reached positions similar to the LIA-limit as  
325 early as ~3 kyr ago. This scenario is supported by several other studies at various sites in the Alps, that  
326 recorded significant glacier advances around that time, based on radiocarbon dating, regionally defined  
327 as the Göschener I Oscillation (~3.0 - 2.3 kyr ago; Zoller et al., 1966; review in Ivy-Ochs et al., 2009).

328

#### 329 5.4 Little Ice Age

330 The fourteen boulder ages on the LIA limit ranging between ~580 yr and 140 yr match the timing of  
331 the LIA (Fig. 4F and 5A) and are remarkably consistent internally with the stratigraphy of the  
332 individual moraines ridges, where such is discernible, i.e. on the Chüebergli (Figs. 1, 2B) and at the  
333 highly resolved moraine sequence close to northern flank of the Bockberg (inset in Fig. 1). We infer  
334 that our LIA age population reflects several glacier maxima within a ~450 yr period, and we will  
335 attempt here to use the resulting  $^{10}\text{Be}$  age distribution to resolve individual glacier culminations during  
336 this interval. A limiting factor to the accuracy of young surface exposure boulder ages is the possible  
337 presence of  $^{10}\text{Be}$  derived from periods of exposure prior to final moraine deposition (hereafter  
338 'inheritance') (cf. Balco, 2011). Our two post-LIA boulders STEI-16 and -7 allow a natural experiment  
339 to test the magnitude of potential inheritance by comparison of their  $^{10}\text{Be}$  ages (~160 yr and ~130 yr,  
340 respectively) with the years of the historically recorded glacier positions (shortly after 1920 CE and

341 1988 CE, respectively) (Fig. 1). These two boulders indicate inheritance on the order of 50-100 yr,  
342 corresponding to as little as  $<2000 \text{ atoms (g quartz)}^{-1}$ . On the other hand, applying a general  
343 inheritance correction by systematically subtracting 50-100 yr from the Steingletscher LIA ages would  
344 render some of them unrealistically young, in particular sample STEI-12-20 ( $140 \pm 34 \text{ yr}$ ). This  
345 implies that whether or not a boulder surface has significant inheritance is random and that the two test  
346 boulders STEI-16 and -7 are probably incidentally affected by an amount of inheritance higher than in  
347 other boulders sampled. Based on these observations and the internal consistency of the LIA boulder  
348 stratigraphy we refrain from applying a general correction, assuming negligible inheritance for our LIA  
349 boulders.

350 We applied three different statistical tests to identify distinct peaks in the LIA age population (Table  
351 3): the visual Kernel Density Estimation using the DensityPlotter published by Vermeesh (2012) (Fig.  
352 5A), the cluster analysis Partitioning Around Medoids (PAM) following Kaufman and Rousseeuw  
353 (1987), and a Chi-square test according to Ward and Wilson (1978). The three different tests yield  
354 similar results (Table 3), suggesting that our distribution of  $^{10}\text{Be}$  ages represents four LIA glacier  
355 culminations around 1470 CE ( $\sim 540 \text{ yr ago}$ ), 1650 CE ( $\sim 360 \text{ yr ago}$ ), 1750 CE ( $\sim 260 \text{ yr ago}$ ) and 1820  
356 CE ( $\sim 190 \text{ yr ago}$ ), indicated by the black arrows in Fig. 5A. Comparing these results with the detailed  
357 LIA chronologies by Holzhauser et al. (2005), we note that the two  $^{10}\text{Be}$  age peaks from Steingletscher  
358 at  $\sim 1650 \text{ CE}$  and  $\sim 1820 \text{ CE}$  match well with the advanced positions of the Swiss glaciers Great Aletsch,  
359 Gorner and Lower Grindelwald, as illustrated in Fig. 5. The two peaks at  $\sim 1470 \text{ CE}$  and  $\sim 1750 \text{ CE}$   
360 have not been reported for Great Aletsch Glacier and Gorner Glacier. However, the higher-resolution  
361 record from Lower Grindelwald Glacier illustrates glacier culminations in the middle of the 18<sup>th</sup>  
362 century in agreement with our peak at  $\sim 1750 \text{ CE}$ . The data gap around the 15<sup>th</sup> century in the Lower

363 Grindelwald Glacier record prevents us from assessing if it experienced glacier advances similar to the  
364 Steingletscher  $^{10}\text{Be}$  age peak around 1470 CE.

365 We conclude that our LIA  $^{10}\text{Be}$  boulder age record, being in chronological order with the individual  
366 moraine ridge stratigraphy, shows good agreement with the independent documentations of LIA  
367 glacier fluctuations in the Alps and that it points to four sub-culminations during the LIA period. The  
368 lower number of advances recorded for the Great Aletsch and Gorner Glaciers might be explained by  
369 longer reaction times of these glaciers. The reaction of a glacier to climate change depends on various  
370 characteristics including size, surface area distribution with altitude, and steepness of the bed (Cuffey  
371 and Paterson, 2010). The most striking difference between the four glaciers compared here is the size  
372 of their surface areas. Small alpine glaciers are more sensitive to short-term climate changes than big  
373 glaciers with reaction times ranging from a few years to several decades (e.g. Holzhauser et al., 2005).  
374 While Aletsch and Gorner glacier are the two largest glaciers in Switzerland with surface areas of 90  
375  $\text{km}^2$  and  $60 \text{ km}^2$ , respectively, Steingletscher and the Lower Grindelwald glacier are much smaller with  
376 surface areas of  $6 \text{ km}^2$  and  $20 \text{ km}^2$  (Glaciological reports, 1881-2009), respectively, and thus likely to  
377 experience more frequent fluctuations on the decadal to centennial time scales considered here.

378

## 379 **6. Conclusions**

380 We present a comprehensive Holocene glacier chronology of Steingletscher, Central Swiss Alps, based  
381 on high-sensitivity  $^{10}\text{Be}$  moraine boulder dating. The  $^{10}\text{Be}$  moraine chronology is consistent with the  
382 moraine ridge stratigraphy and agrees well with independent constraints for the Holocene culminations  
383 of the Steingletscher and with other glacier records in the Alps. The chronology implies that the largest  
384 glacier extents studied at Steingletscher occurred about 11-10 kyr ago, during the Late Glacial/Early  
385 Holocene transition. We do not record any glacier culminations during the mid-Holocene in agreement  
386 with independent findings of a prolonged period of glacial retreat during the mid-Holocene. Several

387 boulder ages around 2.8 kyr corroborate the growing evidence for a significant glacier advance to LIA  
388 extent as early as ~3 kyr ago in the Alps. Fourteen boulder ages, partly derived from unusually small  
389 quartz samples, match with the LIA period. We use these ages for a first attempt to resolve the fine  
390 structure of LIA glacier culminations based on <sup>10</sup>Be dating of moraine boulders. The good agreement  
391 of our results with independent records in the Swiss Alps suggests a high potential of the method to  
392 complement existing historical data and dating approaches.

393

## 394 ACKNOWLEDGEMENTS

395 We thank J. Hanley and K. Needleman for help with sample preparation; A. Putnam, M. Pasturel, L.  
396 Benedetti, and R. Braucher for assistance during data interpretation; and the staff of the Center for  
397 Accelerator Mass Spectrometry at Lawrence Livermore National Laboratory for the excellent  
398 measurements. We acknowledge support by the CRONUS-Earth project (Cosmic-Ray Produced  
399 Nuclide Systematics on Earth) (U.S. National Science Foundation grant EAR-0345835), the  
400 International Balzan Foundation, the German Academic Exchange Service (DAAD), the College de  
401 France, the Lamont Climate Center, the Comer Science and Education Foundation and the Hans-  
402 Sigrist Foundation. We thank Joe Licciardi and an anonymous reviewer for their constructive reviews,  
403 which greatly improved the manuscript. This is Lamont-Doherty Earth Observatory publication xxx.

404

## 405 References:

406

407 Akçar, N., Deline, P., Ivy-Ochs, S., Alfimov, V., Hajdas, I., Kubik, P.W., Christl, M., Schlüchter, C., 2012. The AD 1717  
408 rock avalanche deposits in the upper Ferret Valley (Italy): a dating approach with cosmogenic <sup>10</sup>Be. *Journal of Quaternary*  
409 *Science* 27, 383–392.

410 Alley, R.B., Mayewski, P.A., Sowers, T., Stuiver, M., Taylor, K.C., Clark, P.U., 1997. Holocene climatic instability: A  
411 prominent, widespread event 8200 yr ago. *Geology* 25, 483–486.

412 André M.-F., 2002. Rates of postglacial rock weathering on glacially scoured outcrops (Abisko-Riksgransen Area, 68-N).  
413 *Geografiska Annaler* 84 A, 139–150.

414 Balco, G., Stone, J., Lifton, N., Dunai, T., 2008. A complete and easily accessible means of calculating surface exposure  
415 ages or erosion rates from <sup>10</sup>Be and <sup>26</sup>Al measurements. *Quaternary Geochronology* 3, 174–195.

416 Balco, G., Briner, J., Finkel, R.C., Rayburn, J.A., Ridge, J.C., Schaefer, J.M., 2009. Regional beryllium-10 production rate  
417 calibration for late-glacial northeastern North America. *Quaternary Geochronology* 4, 93–107,  
418 doi:10.1016/j.quageo.2008.09.001.

419 Balco, G., 2011. Contributions and unrealized potential contributions of cosmogenic-nuclide exposure dating to glacier  
420 chronology, 1990–2010. *Quaternary Science Reviews* 30, 3–27, doi:10.1016/j.quascirev.2010.11.003.

421 Baroni, C., Orombelli, G., 1996. The Alpine “Iceman” and Holocene climatic change. *Quaternary Research* 46, 78–83.

422 Blass, A., Anselmetti, F.S., Ariztegui, D., 2003. 60 years of glaciolacustrine sedimentation in Steinsee (Sustenpass,  
423 Switzerland) compared with historic events and instrumental meteorological data. *Eclogae geologicae Helvetiae* 96,  
424 Supplement 1, S59–S71.

- 425 Bronk Ramsey, C., 2009. Bayesian analysis of radiocarbon dates. *Radiocarbon* 51, 337-360.
- 426 Bronk Ramsey, C., 2013. OxCal Program 4.2.3, <https://c14.arch.ox.ac.uk/oxcal/OxCal.html>
- 427 Cossart, E., Fort, M., Bourlès, D., Braucher, R., Perrier, R., Siame, L., 2012. Deglaciation pattern during the  
428 Lateglacial/Holocene transition in the southern French Alps. Chronological data and geographical reconstruction from the  
429 Clarée Valley (upper Durance catchment, southeastern France). *Palaeogeography, Palaeoclimatology, Palaeoecology* 315-  
430 316, 109–123.
- 431 Cuffey, K.M. and Paterson, W.S.B., 2010. *The Physics of Glaciers*. Fourth edition. Butterworth-Heinemann/Elsevier,  
432 Burlington, USA. 693 p.
- 433 Fenton C.R., Hermanns R., Blikra L., Kubik P.W., Bryant C., Niedermann S., Meixner A., Goethals M.M., 2011. Regional  
434 <sup>10</sup>Be production rate calibration for the past 12 ka deduced from the radiocarbon-dated Grøtlandsura and Russenes rock  
435 avalanches at 69° N, Norway. *Quaternary Geochronology* 6, 437–452.
- 436 Glaciological reports, 1881-2009. "The Swiss Glaciers", Yearbooks of the Cryospheric Commission of the Swiss Academy  
437 of Sciences (SCNAT) published since 1964 by the Laboratory of Hydraulics, Hydrology and Glaciology (VAW) of ETH  
438 Zürich. No. 1-126, (<http://glaciology.ethz.ch/swiss-glaciers/>).
- 439 Goehring, B.M., Schaefer, J.M., Schluechter, C., Lifton, N.A., Finkel, R.C., Jull, A.J.T., Akçar, N., Alley, R.B., 2011a. The  
440 Rhone Glacier was smaller than today for most of the Holocene. *Geology* 39, 679-682.
- 441 Goehring B.M., Lohne Ø.S., Mangerud J., Svendsen J.I., Gyllencreutz R., Schaefer J., Finkel R., 2011b. Late Glacial and  
442 Holocene beryllium-10 production rates for western Norway. *Journal of Quaternary Science* 27, 89-96.
- 443 Grove, J.M., 2001. The initiation of the 'Little Ice Age' in regions round the North Atlantic. *Climate Change* 48, 53–82.
- 444 Holzhauser, H., Magny, M., Zumbühl, H.J., 2005. Glacier and lake-level variations in west-central Europe over the last  
445 3500 years. *The Holocene* 15, 789–801, doi:10.1191/0959683605hl853ra.
- 446 Hormes, A., Müller, B.U., Schlüchter, C., 2001. The Alps with little ice: evidence for eight Holocene phases of reduced  
447 glacier extent in the Central Swiss Alps. *The Holocene* 11, 255–265.
- 448 Ivy-Ochs S., Schlüchter C., Kubik P.W., Synal H.-A., Beer J., Kerschner H., 1996. The exposure age of an Egesen moraine  
449 at Julier Pass, Switzerland, measured with the cosmogenic radionuclides <sup>10</sup>Be, <sup>26</sup>Al and <sup>36</sup>Cl. *Eclogae Geologicae Helveticae*  
450 89(3): 1049–1063.
- 451 Ivy-Ochs, S., Kerschner, H., Reuther, A., Maisch, M., Sailer, R., Schaefer, J., Kubik, P., Synal, H., 2006. The timing of  
452 glacier advances in the northern European Alps based on surface exposure dating with cosmogenic <sup>10</sup>Be, <sup>26</sup>Al, <sup>36</sup>Cl, and  
453 <sup>21</sup>Ne. In: Siame, L.L., Bourlès, D.L., Brown, E.T. (Eds.), *In Situ-Produced Cosmogenic Nuclides and Quantification of*  
454 *Geological Processes*. Geological Society of America, Special Paper 415, 43–60.
- 455 Ivy-Ochs, S., Kerschner, H., Maisch, M., Christl, M., Kubik, P. W., Schluechter, C., 2009. Latest Pleistocene and Holocene  
456 glacier variations in the European Alps. *Quaternary Science Reviews* 28, 2137–2149.
- 457 Joerin, U.E., Stocker, T.F., Schlüchter, C., 2006. Multicentury glacier fluctuations in the Swiss Alps during the Holocene:  
458 *The Holocene* 16, 697–704, doi:10.1191/0959683606hl964rp.
- 459 Joerin, U.E., Nicolussi, K., Fischer, A., Stocker, T.F., Schlüchter, C., 2008. Holocene optimum events inferred from  
460 subglacial sediments at Tschierva Glacier, Eastern Swiss Alps. *Quaternary Science Reviews* 27, 337–350.
- 461 Kaufman L., Rousseeuw, P., 1987. Clustering by Means of Medoids. In Y. Dodge (Ed.) *Statistical Data Analysis Based on*  
462 *the L1-Norm and Related Methods*, pp. 405–416. North-Holland.
- 463 Kelly, M.A., Kubik, P.W., Blanckenburg von, F., Schlüchter, C., 2004. Surface exposure dating of the Great Aletsch  
464 Glacier Egesen moraine system, western Swiss Alps, using the cosmogenic nuclide <sup>10</sup>Be. *Journal of Quaternary Science* 19,  
465 431–441.
- 466 King, L., 1974. Studien zur postglazialen Gletscher- und Vegetationsgeschichte des Sustenpassgebietes. *Baseler Beiträge*  
467 *zur Geographie* 18, 1–123.
- 468 Licciardi, J.M., Schaefer, J.M., Taggart, J.R., Lund, D.C., 2009. Holocene glacier fluctuations in the Peruvian Andes  
469 indicate northern climate linkages. *Science* 325, 1677–1679, doi:10.1126/science.1175010.

- 470 Lal, D., 1991. Cosmic ray labeling of erosion surfaces: in situ nuclide production rates and erosion models. *Earth and*  
471 *Planetary Science Letters* 104, 424-439, doi: 10.1016/0012-821X(91)90220-C.
- 472 Nicolussi, K., Schlüchter, C., 2012. The 8.2 ka event—Calendar-dated glacier response in the Alps. *Geology* 40, 819-822.
- 473 Nishiizumi K., Imamura M., Caffee M.W., Southon, J.R., Finkel, R.C., McAninch, J., 2007. Absolute calibration of  $^{10}\text{Be}$   
474 AMS standards. *Nuclear Instruments and Methods in Physics Research Section B: Beam Interactions with Materials and*  
475 *Atoms* 258, 403–413.
- 476 Oerlemans, J., 2005. Extracting a Climate Signal from 169 Glacier Records. *Science* 308, 675-677.
- 477 Putnam A.E., Schaefer J.M., Barrell D.J.A., Vandergoes M., Denton G.H., Kaplan M.R., Finkel R.C., Schwartz R.,  
478 Goehring B.M., Kelley S.E., 2010. In situ cosmogenic  $^{10}\text{Be}$  production-rate calibration from the Southern Alps, New  
479 Zealand. *Quaternary Geochronology* 5, 392–409.
- 480 Rasmussen, S.O., Vinther, B.M., Clausen, H.B., Andersen, K.K., 2007. Early Holocene climate oscillations recorded in  
481 three Greenland ice cores. *Quaternary Science Reviews* 26, 1907–1914, doi:10.1016/j.quascirev.2007.06.015.
- 482 Rasmussen, S.O., Andersen, K.K., Svensson, A.M., Steffensen, J.P., Vinther, B.M., Clausen, H.B., Siggaard-Andersen, M.-  
483 L., Johnsen, S.J., Larsen, L.B., Dahl-Jensen, D., Bigler, M., Röthlisberger, R., Fischer, H., Goto-Azuma, K., Hansson, M.  
484 E., Ruth, U., 2006. A new Greenland ice core chronology for the last glacial termination. *Journal of Geophysical Research*  
485 111, D06102, doi:10.1029/2005JD006079.
- 486 Reimer, P.J., Bard, E., Bayliss, A., Beck, J.W., Blackwell, P.G., Bronk Ramsey, C., Grootes, P.M., Guilderson, T.P.,  
487 Hafliðason, H., Hajdas, I., Hatté, C., Heaton, T.J., Hoffmann, D.L., Hogg, A.G., Hughen, K.A., Kaiser, K.F., Kromer, B.,  
488 Manning, S.W., Niu, M., Reimer, R.W., Richards, D.A., Scott, E.M., Southon, J.R., Staff, R.A., Turney, C.S.M., van der  
489 Plicht, J., 2013. IntCal13 and Marine13 Radiocarbon Age Calibration Curves 0-50,000 Years cal BP. *Radiocarbon* 55,  
490 1869-1887.
- 491 Röthlisberger, F., Schneebeli, W., 1979. Genesis of lateral moraine complexes, demonstrated by fossil soils and trunks:  
492 Indicators of postglacial climatic fluctuations, in Schlüchter, C., ed., *Moraines and varves*. Rotterdam, A.A. Balkema, pp.  
493 387–419.
- 494 Schaefer, J.M., Denton, G.H., Kaplan, M., Putnam, A., Finkel, R.C., Barrell, D.J.A., Andersen, B.G., Schwartz, R.,  
495 Mackintosh, A., Chinn, T., Schlüchter, C., 2009. High-frequency Holocene glacier fluctuations in New Zealand differ from  
496 the northern signature. *Science*, 324, 622– 625, doi:10.1126/science.1169312.
- 497 Schimmelpfennig, I., Schaefer, J.M., Akçar, N., Ivy-Ochs, S., Finkel, R.C., Schlüchter, C., 2012. Holocene glacier  
498 culminations in the Western Alps and their hemispheric relevance. *Geology* 40, 891-894, doi:10.1130/G33169.1.
- 499 Schindelwig, I., Akçar, N., Kubik, P.W., Schlüchter, C., 2012. Lateglacial and early Holocene dynamics of adjacent valley  
500 glaciers in the Western Swiss Alps. *Journal of Quaternary Science*, 27, 114–124, doi:10.1002 /jqs.1523.
- 501 Schwander, J., Eicher, U., Ammann, B., 2000. Oxygen isotopes of lake marl at Gerzensee and Leysin (Switzerland),  
502 covering the Younger Dryas and two minor oscillations, and their correlation to the GRIP ice core. *Palaeogeography,*  
503 *Palaeoclimatology, Palaeoecology*, 159, 203–214, doi:10.1016/S0031-0182(00)00085-7.
- 504 Severinghaus, J.P., Beaudette, R., Headly, M. A., Taylor, K., Brook, E.J., 2009. Oxygen-18 of  $\text{O}_2$  Records the Impact of  
505 Abrupt Climate Change on the Terrestrial Biosphere. *Science* 324, 1431-1434.
- 506 Vermeesh, P., 2012. On the visualisation of detrital age distributions. *Chemical Geology* 312-313, 190-194.
- 507 Vinther, B.M., Clausen, H.B., Johnsen, S.J., Rasmussen, S.O., Andersen, K.K., Buchardt, S.L., Dahl-Jensen, D., Seierstad,  
508 I.K., Siggaard-Andersen, M.-L., Steffensen, J.P., Svensson, A., Olsen, J., Heinemeier, J., 2006. A synchronized dating of  
509 three Greenland ice cores throughout the Holocene. *J. Geophys. Res.* 111, D13102, doi:10.1029/2005JD006921.
- 510 Ward, G.K., Wilson, S.R., 1978. Procedures for comparing and combining radiocarbon age-determinations – Critique.  
511 *Archaeometry* 20, 19-31.
- 512 Young, E.Y., Schaefer, J.M., Briner, J.P., Goehring, B.M., 2013. A  $^{10}\text{Be}$  production-rate calibration for the Arctic: *Journal*  
513 *of Quaternary Science* 28, 515-526.
- 514 Zoller, H., 1958. Pollenanalytische Untersuchungen im unteren Misox mit den ersten Radiokarbonatierungen in der  
515 Südschweiz. *Veröffentlichungen des Geobotanischen Instituts Rübél* 34, 166–175.

516 Zoller, H., 1960. Pollenanalytische Untersuchungen zur Vegetationsgeschichte der insubrischen Schweiz. Denkschriften  
517 der Schweizerischen Naturforschenden Gesellschaft 83, 45–156.

518 Zoller, H., Schindler, C., Röthlisberger, 1966. Postglaziale Gletschstände und Klimaschwankungen im Gotthardmassiv und  
519 Vorderrheingebiet. Verhandlungen der Naturforschungs Gesellschaft Basel 77, 97–164.

520

## 521 **Figure Captions and Tables:**

522

523 **Fig. 1:** Map of Holocene moraines and  $^{10}\text{Be}$  boulder ages at Steingletscher (Central Swiss Alps, 47°N  
524 latitude) on ALTI3D model by Swisstopo® (left panel). LIA: Little Ice Age; CE: Common Era. Inset  
525 (A) highlights study area in red.  $^{10}\text{Be}$  ages (in years before 2010 CE) are shown in white boxes with  $1\sigma$   
526 errors including analytical and  $^{10}\text{Be}$  production rate uncertainties and followed by sample names in  
527 orange. Outliers are in italic. Inset (B) shows detail of LIA and post-LIA moraine sequence in the north  
528 of the Bockberg mountain. Pink boxes give years of historically recorded moraine deposits (Fig. 3).  
529 Blue boxes show calibrated bracketing radiocarbon ages (in years before 2010 CE for comparison with  
530  $^{10}\text{Be}$  ages) obtained by King (1974) from the peat bog profiles or fossil soils in outcrops, followed by  
531 profile or outcrop name. Black numbers are maximum ages, and white numbers are minimum ages for  
532 moraine deposits or glacier retreats/advances. Yellow numbers are ages associated with certain pollen  
533 assemblages. For relationship with moraines and climate significance see Table 2. Panel (C) shows  
534 part of the moraine map produced by King (1974) (modified). The original German legend and labels  
535 are translated. Colored numbers are mean  $^{10}\text{Be}$  moraine ages inferred in our study. “Gö2” refers to the  
536 Göschener II Oscillation, a cold phase in the middle of the 1<sup>st</sup> millennium CE regionally defined by  
537 Zoller et al. (1966) (Ivy-Ochs et al., 2009 and references therein).

538

539 **Fig. 2:** Photographs of moraines and related geomorphic features at Steingletscher. A: View of glacier  
540 forefield showing the proglacial lake Steinsee, partly encircled by the LIA limit. B: On the top of hill  
541 Chüebergli, view on the sharp LIA crest with boulder STEI-17, embedded in a slightly inboard located  
542 sub-ridge. C: Part of the inner moraine relicts on the Hublen plateau. In the back, view on the visible  
543 LIA limit and the right-lateral LIA composite moraine. D: Moraine deposited in the year 1988 with  
544 boulder STEI-7. E: Sequence of interlaced individual LIA moraine ridges in the north of Bockberg  
545 mountain.

546

547 **Fig. 3:** Post-LIA length measurements of Steingletscher between the years 1893 and 2011  
548 (Glaciological reports, 1881-2009). The reference length 0 m corresponds to the glacier length in the  
549 first measurement year. During this period, two significant re-advance (blue arrows) ended in the years  
550 1920 and 1988, both followed by decadal retreats (red arrows).

551

552 **Fig. 4:** Holocene glacier culminations of Steingletscher (Central Swiss Alps) based on  $^{10}\text{Be}$  moraine  
553 ages (grey panel F, this study) compared to independent climate records in Greenland and Switzerland  
554 and to other documentations of glacier variations in the European Alps based on  $^{10}\text{Be}$  moraine dating.  
555 Glacier sites are sorted from west to east as depicted by red dots in the inset map. Reference year 0  
556 corresponds to 2010 Common Era. LIA: Little Ice Age. YD: Younger Dryas. Each mean  $^{10}\text{Be}$  moraine  
557 age is represented by a summed probability curve with the number of averaged boulder ages indicated  
558 by  $n=x$ . Only analytical errors are taken into account in the probability curves. Colors represent the  
559 stratigraphic order of the moraine ridges at each site, from outer to inner: red-blue-green-yellow-violet.  
560 Vertical lines inside each curve are the arithmetic means of each moraine age, and colored bands inside

561 the curves are  $1\sigma$  errors including the production rate uncertainty. A: Oxygen-isotope record from  
562 NGRIP ice core in Greenland (Vinther, et al., 2006; Rasmussen et al., 2006) with YD stadial and Early  
563 Holocene cold spells highlighted by grey vertical bands. B: Oxygen-isotope records in sediment cores  
564 of the two Swiss lakes Gerzensee and Leysin (Schwander et al., 2000). Locations are represented by  
565 blue dots in inset map. Panels C-E and H show Glacier culminations based on recalculated  $^{10}\text{Be}$   
566 moraine ages. C: Tsidjiore Nouve Glacier (Western Swiss Alps) (Schimmelpfennig et al., 2012). D:  
567 Belalp Glacier (Western Swiss Alps) (Schindelwig et al., 2012). E: Left-lateral moraine of Great  
568 Aletsch Glacier (Western Swiss Alps) (Kelly et al., 2004). The same panel shows Late Holocene  
569 glacier fluctuations of Great Aletsch Glacier based on  $^{14}\text{C}$ -dating, dendrochronologic analysis,  
570 archeological and historical data (Holzhauser et al., 2005). G: Glacier and climate variations at  
571 Steingletscher based on calibrated bracketing  $^{14}\text{C}$  ages from peat bogs and outcrops at Steingletscher  
572 (King, 1974; Fig. 1; Table 2). Arrows pointing to the right stand for minimum ages, arrows pointing to  
573 the left stand for maximum ages. The arrow lengths correspond to the  $2\sigma$  intervals of calibrated  $^{14}\text{C}$   
574 ages. The arrows are vertically sorted according to the distance of the peat bog or outcrop locations  
575 from the LIA limit (outer to inner). Plain arrows indicate bracketing ages for moraine deposits or  
576 glacier retreats/advances. Dashed arrows correspond to climate cooling (black) or warming (grey)  
577 interpreted from pollen assemblages. H: Kartell site moraine (Eastern Alps, Austria) (Ivy-Ochs et al.,  
578 2006).

579  
580 **Fig. 5:** Comparison of Little Ice Age (LIA) glacier records in the Swiss Alps. CE: Common Era. A:  
581 Probability Density Plot (PDP, thick curve) and Kernel Density Estimation (KDE, blue area;  
582 bandwidth 30 yr; Vermeesh, 2012) of LIA  $^{10}\text{Be}$  boulder ages at Steingletscher (this study). Individual  
583 ages and analytical errors are represented by thin Gauss curves. Arrows indicate timing of KDE peaks.  
584 For comparison with the other glacier records, arrows are vertically extended by grey bands. B: Glacier  
585 fluctuations of the three Swiss glaciers Great Aletsch (upper curve), Gorner (middle curve), and Lower  
586 Grindelwald (lower curve) based on  $^{14}\text{C}$ -dating, dendrochronologic analysis, archeological and  
587 historical data (Holzhauser et al., 2005).  
588

**Table 1:** Sample details, analytical data and surface exposure ages.  $^{10}\text{Be}/^9\text{Be}$  ratios, measured at the Center for Accelerator Mass Spectrometry of the Lawrence Livermore National Laboratory, were normalized to standard 07KNSTD with the  $^{10}\text{Be}/^9\text{Be}$  ratio  $2.85 \times 10^{-12}$  (Nishiizumi et al., 2007). The ages are calculated using the ‘Arctic’  $^{10}\text{Be}$  production rate with a value of  $3.96 \pm 0.15$  atoms  $(\text{g yr})^{-1}$  at sea level/high latitude (Young et al. 2013, normalized to standard 07KNSTD) and the scaling method ‘Lm’ (time-dependent version of Lal, 1991) according to Balco et al. (2008). We assumed standard atmospheric pressure and a rock density of  $2.7 \text{ g cm}^{-3}$ . The rock density is needed to calculate the cosmic ray flux attenuation below the sample surface and thus to integrate the depth-dependent  $^{10}\text{Be}$  production rate over the sample thickness. The local  $^{10}\text{Be}$  production rate of each sample is for spallation only. Note that the local time-integrated production rate scaled with the time-dependent Lm model is not a default output in the CRONUS online calculator (Balco et al., 2008), but time-variable production rates as a function of 500- to 1000-year time steps are provided in a separate file when calculating individual samples. Here, these data points were averaged over the respective rough exposure duration of each sample, and must therefore be considered approximate values. All ages are reported in calendar years before 2010 CE. Outliers are in *italic*.

Sample name	Latitude (°N)	Longitude (°E)	Elevation (m)	Thickness (cm)	Shielding factor	Qtz weight (g)	Carrier (mg $^9\text{Be}$ )	CAMS number	$^{10}\text{Be}/^9\text{Be}$ $\times 10^{14}$	Blank correction	$^{10}\text{Be}$ ( $\times 10^3$ atoms $\text{g}^{-1}$ )	Local $^{10}\text{Be}$ production rate (atoms $\text{g}^{-1} \text{yr}^{-1}$ )	$^{10}\text{Be}$ age (years)	1 $\sigma$ Analyt. error	1 $\sigma$ error incl. prod. rate error
<b>EARLY HOLOCENE</b>															
STEL-27	46.72616	8.42472	2069	1.10	0.985	10.05	0.18401	BE33378	18.99±0.35	0.13%	232.2±4.3	21.0	10860	200 (1.9%)	460
STEL-11	46.72672	8.42504	2059	1.68	0.985	25.18	0.18371	BE31216	45.92±0.86	0.15%	223.6±4.1	20.7	10580	200 (1.9%)	450
STEL-8	46.72613	8.42551	2056	4.10	0.981	20.00	0.18883	BE32356	34.21±0.85	0.04%	215.8±5.4	20.2	10490	260 (2.5%)	480
STEL-9	46.72622	8.42556	2054	2.13	0.981	15.15	0.18381	BE31220	26.60±0.76	0.11%	215.5±6.1	20.5	10320	290 (2.8%)	490
STEL-10	46.72657	8.42552	2055	2.81	0.981	15.54	0.18811	BE32357	25.78±0.60	0.06%	208.4±4.9	20.4	10030	230 (2.3%)	450
STEL-19	46.73062	8.42564	1871	1.75	0.958	49.24	0.18360	BE32380	72.77±1.10	0.06%	181.2±2.7	17.6	10090	150 (1.5%)	410
STEL-20	46.73031	8.42591	1878	1.58	0.957	48.96	0.18360	BE32381	67.80±0.58	0.06%	169.8±1.5	17.7	9395	81 (0.9%)	370
STEL-21	46.73002	8.42624	1884	2.94	0.958	49.83	0.18422	BE32382	60.90±0.61	0.07%	150.4±1.5	17.6	8354	83 (1.0%)	330
<b>LATE HOLOCENE</b>															
STEL-25	46.73083	8.42944	1908	2.01	0.939	20.02	0.18258	BE33352	8.43±0.17	0.22%	51.23±1.05	17.4	2874	59 (2.0%)	120
STEL-22	46.72979	8.42671	1880	3.08	0.958	10.03	0.18391	BE33377	4.136±0.090	0.59%	50.4±1.1	17.2	2852	63 (2.2%)	130
STEL-12	46.73154	8.42342	1838	3.49	0.950	24.64	0.18422	BE31217	9.66±0.18	0.72%	47.93±0.91	16.5	2832	54 (1.9%)	120
STEL-14	46.73155	8.42370	1840	1.88	0.950	30.12	0.18801	BE32359	11.27±0.21	0.66%	46.71±0.89	16.7	2721	52 (1.9%)	120
STEL-13	46.73152	8.42353	1839	2.42	0.950	11.69	0.18780	BE32358	4.33±0.12	0.35%	46.3±1.2	16.7	2711	73 (2.7%)	130
STEL-24	46.73081	8.42966	1916	1.13	0.954	58.17	0.15575	BE32378	18.49±0.37	0.18%	33.02±0.66	17.8	1806	36 (2.0%)	77
<b>LITTLE ICE AGE</b>															
STEL-12-23	46.71618	8.42957	2105	1.53	0.968	8.70	0.1805	BE34659	0.880±0.069	2.56%	12.2±1.0	20.4	580	48 (8.3%)	53
STEL-23	46.73085	8.42980	1915	1.31	0.954	69.09	0.15524	BE32572	6.50±0.13	0.52%	9.71±0.20	17.6	538	11 (2.0%)	23
STEL-12-13	46.71505	8.43060	2139	1.62	0.957	25.37	0.1806	BE34688	2.325±0.083	0.74%	11.24±0.41	20.6	530	19 (3.6%)	28
STEL-26	46.73069	8.42932	1901	1.59	0.951	24.30	0.18452	BE33353	1.659±0.078	1.13%	8.32±0.40	17.3	468	23 (4.9%)	29
STEL-12-05	46.71407	8.43092	2167	2.19	0.928	15.14	0.1809	BE34686	0.976±0.057	2.25%	7.80±0.47	20.3	373	23 (6.2%)	27
STEL-12-14	46.71532	8.43042	2131	4.33	0.960	7.06	0.1796	BE34657	0.443±0.037	5.10%	7.32±0.70	20.1	353	35 (9.6%)	36
STEL-18	46.72112	8.42968	2037	2.06	0.960	69.34	0.15442	BE32571	4.17±0.11	0.81%	6.16±0.17	19.2	313	8 (2.6%)	15
STEL-15	46.71848	8.43005	2128	3.15	0.960	43.81	0.15380	BE32377	2.51±0.10	1.65%	5.78±0.24	20.3	278	11 (4.0%)	15
STEL-12-21	46.71605	8.43005	2112	4.75	0.967	20.01	0.1801	BE34658	0.905±0.057	2.49%	5.43±0.36	20.0	264	18 (6.8%)	20
STEL-12-11	46.71475	8.43090	2149	2.96	0.944	10.13	0.1805	BE34639	0.454±0.038	7.60%	5.11±0.48	20.2	245	23 (9.4%)	25
STEL-12-07	46.71445	8.43102	2149	1.51	0.935	7.02	0.1817	BE34687	0.259±0.029	8.45%	4.20±0.54	20.4	200	26 (13.0%)	27
STEL-12-04	46.71410	8.43137	2164	1.76	0.929	7.99	0.1816	BE34685	0.282±0.029	7.77%	4.04±0.47	20.4	192	22 (11.5%)	24
STEL-17	46.71948	8.43042	2109	2.78	0.976	70.76	0.15452	BE32570	2.78±0.11	1.22%	4.01±0.16	20.5	191	7 (3.7%)	10
STEL-12-20	46.71575	8.430267	2118	2.93	0.965	15.16	0.1807	BE34693	0.052±0.019	12.8%	2.95±0.70	20.3	140	34 (24.3%)	34
<b>POST-LITTLE ICE AGE</b>															
STEL-16	46.71830	8.43105	2100	2.08	0.966	72.20	0.15380	BE32569	2.40±0.11	1.42%	3.37±0.16	20.3	162	8 (4.9%)	10
STEL-7	46.72326	8.43268	1936	4.14	0.934	52.14	0.12462	BE32566	1.421±0.071	1.79%	2.23±0.11	17.1	127	7 (5.5%)	8
Blank name	Processed with								Total number of atoms $^{10}\text{Be}$ $\times 10^3$						
Blank_2_2011Jan18	STEL-11, -12								0.18371	BE31218	0.069±0.015	8.5±1.8			
Blank_1_2011Jan18	STEL-9								0.18493	BE31221	0.030±0.010	3.7±1.2			
Blank_1_2011Sep07	STEL-8, -10, -13								0.18708	BE32365	0.015±0.009	1.9±1.2			
Blank_2_2011Sep07	STEL-14								0.18657	BE32565	0.075±0.024	9.4±3.0			
Blank_1_2011Oct4	STEL-7								0.12380	BE32567	0.026±0.016	2.1±1.3			
Blank_1_2011Nov4	STEL-15								0.15524	BE32379	0.041±0.012	4.2±1.3			
Blank_2_2011Nov4	STEL-16, -17, -18, -23, -24								0.15544	BE32573	0.034±0.015	3.5±1.5			
Blank_3_2011Nov4	STEL-19, -20, -21								0.18391	BE32383	0.044±0.014	5.4±1.7			
Blank_1_2012Feb02	STEL-22, -27								0.18483	BE33381	0.022±0.007	2.76±0.86			
Blank_2_2012Feb02	STEL-22, -27								0.18493	BE33382	0.026±0.008	3.24±0.98			
Blank_2_2012Apr06	STEL-25, -26								0.18504	BE33351	0.019±0.001	2.3±1.2			
Blank_1_2013Jan11	STEL-12-04, -								0.1810	BE34684	0.022±0.009	2.7±1.1			

Blank_2_2013Jan11	05,-07				
Blank_1_2013Jan24	STEI-12-13	0.1808	BE34691	0.017±0.008	2.11±0.99
Blank_2_2012Dec21	STEI-12-20	0.1837	BE34698	0.052±0.019	6.6±2.4
Blank_4_2013Jan11	STEI-12-11	0.1811	BE34642	0.034±0.012	4.3±1.5
	STEI-12-14, -	0.1802	BE34656	0.023±0.016	2.8±2.0
	21,-23				

---

**Table 2:** Bracketing radiocarbon ages from peat bog profiles or fossil soils in outcrops at Steingletscher, determined by King (1974), and their glacier-climatic significance. Sample locations are indicated in Fig. 1. All calibrated ages are given as  $2\sigma$  intervals, reported relative to the years 1950 CE and 2010 CE (for comparison with  $^{10}\text{Be}$  ages). They are calibrated with OxCal 4.2.3 (Bronk Ramsey, 2009, 2013) relative to the IntCal13 calibration data set (Reimer et al., 2013).

Sample number	Profile and sample name	$^{14}\text{C}$ age, uncalibrated (yr)	Calibrated age, $2\sigma$ interval (yr before 1950 CE)	Calibrated age, $2\sigma$ interval (yr before 2010 CE) <sup>1</sup>	Location	Dated material	Significance
B-2292	ST5 - Basisprobe	9200 ± 100	10650 – 10199	<b>10710 – 10259</b>	Peat bog about 300 m outboard of lower Early Holocene moraine on plateau 'In Miseren', presumably inboard of glacier position that corresponds to higher Early Holocene moraines on plateau 'Hublen'	Organic material from near base of peat bog	Minimum age for deglaciation of plateau 'In Miseren'; according to King (1974) minimum age for glacier retreat after deposition of higher Early Holocene moraines on plateau 'Hublen'
B-2293	ST1 - Basisprobe	8320 ± 380	10234 – 8411	<b>10294 – 8471</b>	Peat bog on plateau 'Hublen' directly outboard of outmost moraine in the sequence	Lowest gyttja in peat bog (only small amounts of organic material)	Minimum age for glacier retreat from this position
B-2289	ST8 - Basisprobe	8090 ± 110	9395 – 8636	<b>9455 – 8696</b>	Peat bog about 25 m outboard of lower Early Holocene moraine on plateau 'In Miseren'; no direct relationship with moraine	Organic material from base of peat bog	Minimum age for deglaciation of plateau 'In Miseren'; according to King (1974) pollen assemblage corresponding to this date implies maybe warmer climate afterwards
B-2378	ST9 - Basisprobe	6700 ± 110	7788 – 7420	<b>7848 – 7480</b>	Peat bog directly outboard of lower Early Holocene moraine on plateau 'In Miseren'; peat bog was dammed by moraine	Organic material from base of peat bog	Minimum age for adjacent moraine, because moraine dammed peat bog
B-2291	ST5 - Abiesanstieg	6380 ± 100	7482 – 7024	<b>7542 – 7084</b>	Peat bog about 300 m outboard of lower Early Holocene moraine on plateau 'In Miseren', presumably inboard of glacier position that corresponds to higher Early Holocene moraines on plateau 'Hublen'	Organic material in lower part of profile	Based on pollen assemblage: King assumes that this date marks the end of a slightly 'colder' phase (maybe 'Misox Oscillation' <sup>2</sup> )
B-2290	ST5 - Piceaanstieg	4840 ± 100	5876 – 5320	<b>5936 – 5380</b>	Peat bog about 300 m outboard of lower Early Holocene moraine on plateau 'In Miseren', presumably inboard of glacier position that corresponds to higher Early Holocene moraines on plateau 'Hublen'	Organic material in middle part of profile	Based on pollen assemblage: King assumes warm climate before this date and a longer period (~3000 years) of 'unstable' climate including several cold excursions afterwards (maybe including the 'Göschener 1 Oscillation' <sup>3</sup> )
B-2516	Grabung D	3490 ± 70	3961 - 3588	<b>4021 - 3648</b>	Outcrop dug on right-lateral side on slope of cliff; directly outboard of oldest moraine on 'LIA limit'	Soil material from uppermost part of fossil A-horizon, overtopped by glacial sediment	Maximum age for adjacent moraine deposit
B-2287	Hotel 2, über Fels	3040 ± 100	3454 – 2955	<b>3514 – 3015</b>	In basement of 'Hotel'	Decomposed organic matter below fluvioglacial sediments	Maximum age for glacier advance
B-2288	Hotel 1 - Basisprobe	2820 ± 130	3339 – 2737	<b>3399 – 2797</b>	In basement of 'Hotel'	Organic material from base of peat profile	Minimum age for glacier retreat from this position
B-2286	Steinalp - Basisprobe	2210 ± 100	2461 – 1946	<b>2521 – 2006</b>	Profile dug on right-lateral side, at valley bottom close to river; a few meters outboard of 'LIA limit'	Wood fragment from base of peat that lies on fluvioglacial sediments	Minimum age for glacier retreat from this position

<sup>1</sup> We added 60 years to the calibrated radiocarbon ages to synchronize with the  $^{10}\text{Be}$  ages, which are referenced to 2010 CE.

<sup>2</sup> The 'Misox Oscillation' has regionally been defined by Zoller (1958, 1960) and dated to about 7500 - 6500  $^{14}\text{C}$ - years ago (~8.4-7.3 cal kyr, Ivy-Ochs et al., 2009), based on pollen profiles; this cold oscillation might include the 8.2 kyr. event identified in Greenland ice cores and other paleoclimate records (e.g. Alley et al., 1997).

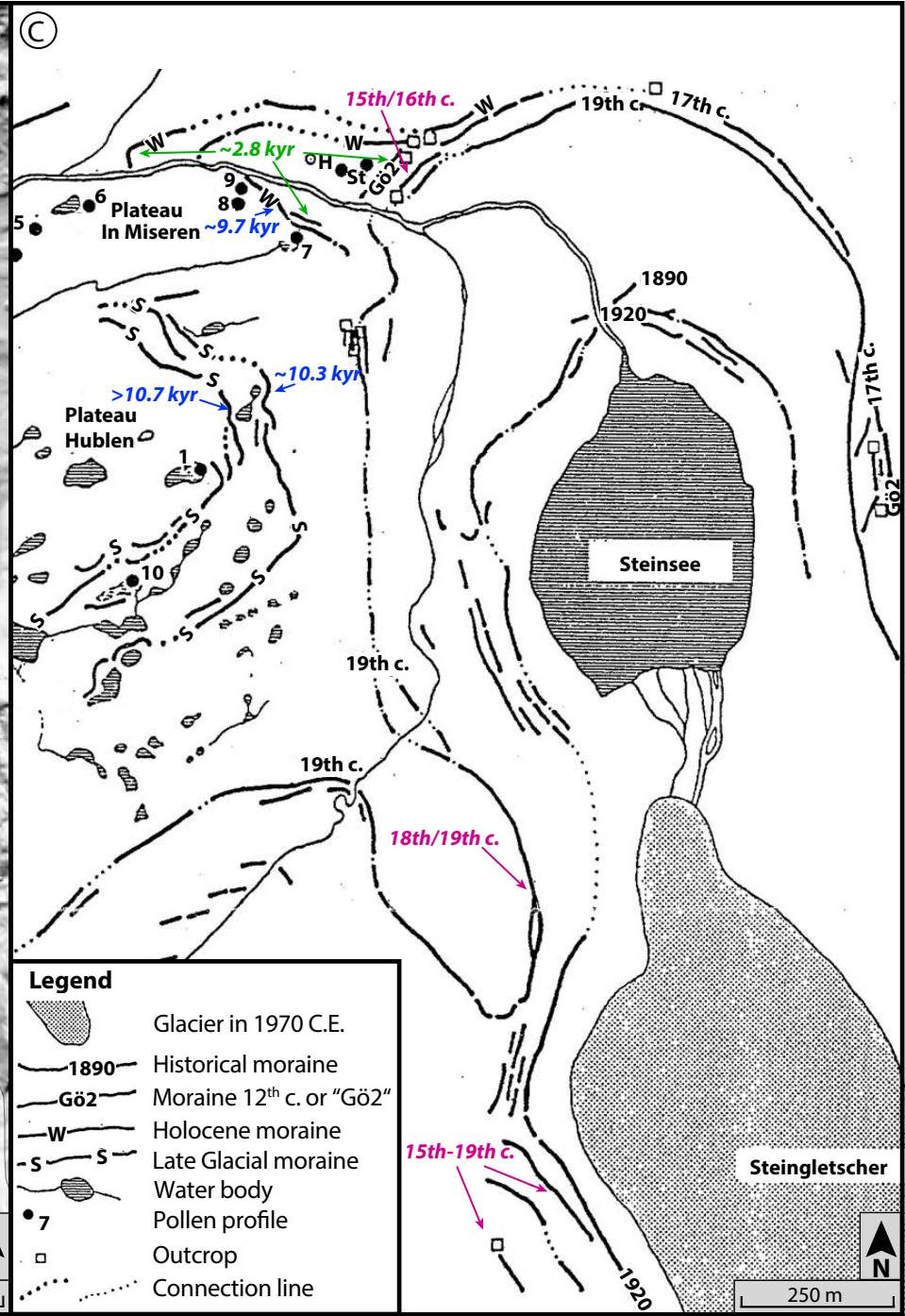
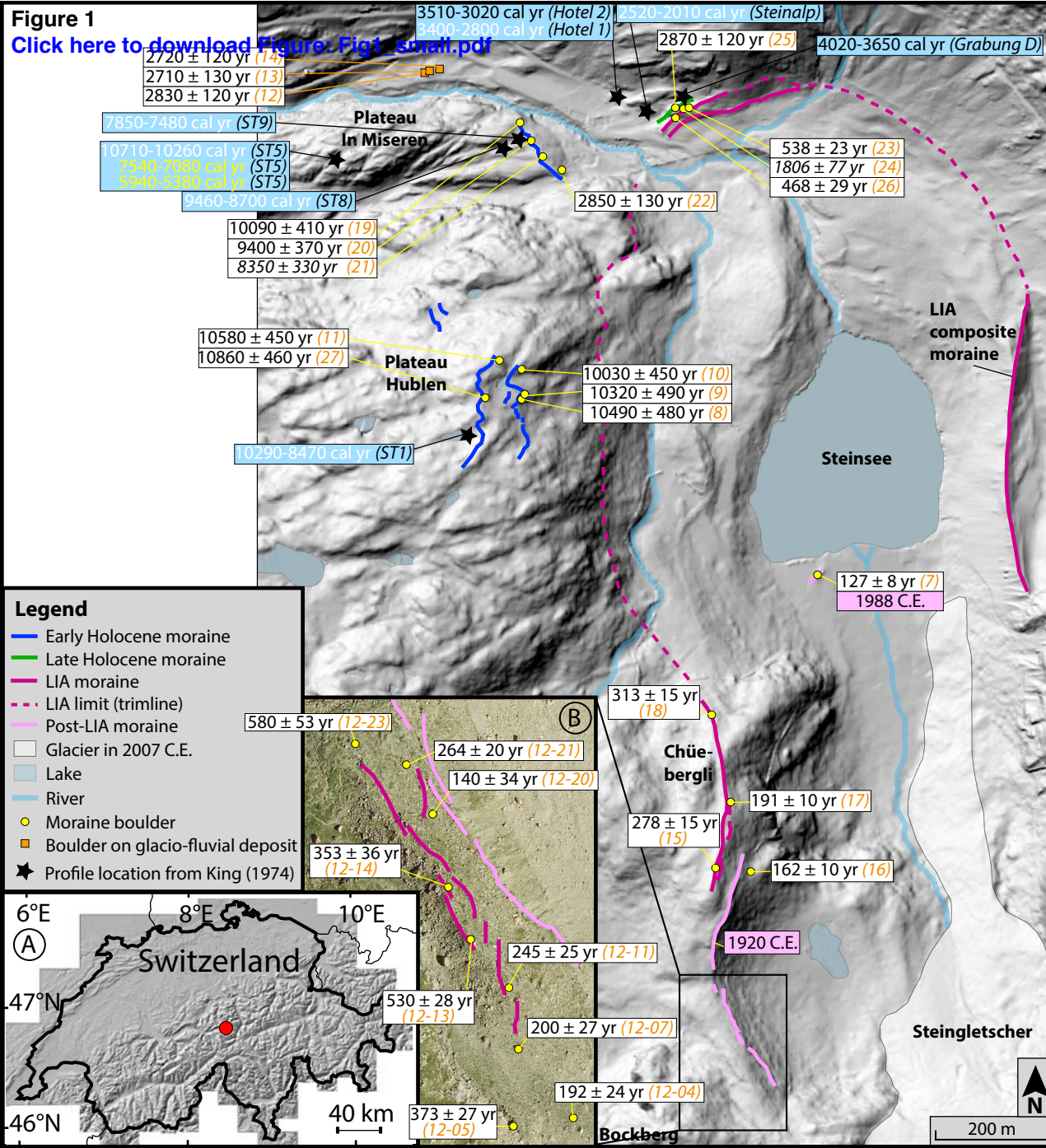
<sup>3</sup> The 'Göschener 1 Oscillation' has regionally been defined by Zoller et al., (1966) and dated to about 2900 – 2300  $^{14}\text{C}$ - years ago (~3.0-2.3 cal kyr, Ivy-Ochs et al., 2009), based on pollen profiles.

**Table 3:** Results of statistical tests on the Little Ice Age  $^{10}\text{Be}$  age distribution at Steingletscher to identify age groups that might represent individual glacier culminations. Mean ages from the Kernel Density Estimation (KDE) are visually inferred from the plot in Fig. 3A, generated using DensityPlotter published by Vermeesh (2012) with a bandwidth of 30 years. Analytical uncertainties in the ages are not taken into account in the KDE. The cluster analysis Partitioning Around Medoids (PAM) follows Kaufman and Rousseeuw (1987); it does not account for the age uncertainties. The results of the PAM test indicate that STEI-18 might belong to group 2, but is dissimilar with the other ages in group 2, and is therefore not included in the mean age. The Chi-square test takes into account the analytical uncertainties, following Ward and Wilson (1978). STEI-26 and STEI-18 do not fit in group 1 and group 2, respectively, and are not included in the respective mean ages.

Sample	$^{10}\text{Be}$ age $\pm$ analytical error (years ago)	Age groups	Kernel Density Estimation peak age (years before 2010 CE) and corresponding year CE	cluster analysis PAM mean age $\pm$ standard deviation (years before 2010 CE) and corresponding year CE	Chi-square test Error-weighted mean age $\pm$ error-weighted standard deviation (years before 2010 CE) and corresponding year CE
STEI-12-23	580 $\pm$ 48	Group 1	540 years ago (1470 CE)	529 $\pm$ 46 years ago (1481 CE)	538 $\pm$ 9 years ago (1472 CE)
STEI-23	538 $\pm$ 11				
STEI-12-13	530 $\pm$ 19				
STEI-26	468 $\pm$ 23				
STEI-12-05	373 $\pm$ 23	Group 2	348 years ago (1662 CE)	363 $\pm$ 14 years ago (1647 CE)	367 $\pm$ 19 years ago (1643 CE)
STEI-12-14	353 $\pm$ 34				
STEI-18	313 $\pm$ 8				
STEI-15	278 $\pm$ 11	Group 3	258 years ago (1752 CE)	262 $\pm$ 17 years ago (1748 CE)	270 $\pm$ 9 years ago (1740 CE)
STEI-12-21	264 $\pm$ 18				
STEI-12-11	245 $\pm$ 23				
STEI-12-07	200 $\pm$ 26	Group 4	200 years ago (1810 CE)	181 $\pm$ 27 years ago (1829 CE)	190 $\pm$ 6 years ago (1820 CE)
STEI-12-04	192 $\pm$ 22				
STEI-17	191 $\pm$ 7				
STEI-12-20	140 $\pm$ 34				

- We present a comprehensive Holocene moraine chronology from the Central Swiss Alps.
- Early Holocene advances are nearly synchronous with those elsewhere in the Alps.
- Late Holocene  $^{10}\text{Be}$  boulder ages suggest a significant glacier advance  $\sim 3$  kyr ago.
- Fourteen of the youngest boulder ages resolve four Little Ice Age glacier peaks.
- LIA boulder ages are partly derived from quartz weights as little as 7-20 g.

**Figure 1**  
[Click here to download Figure: Fig1\\_small.pdf](#)



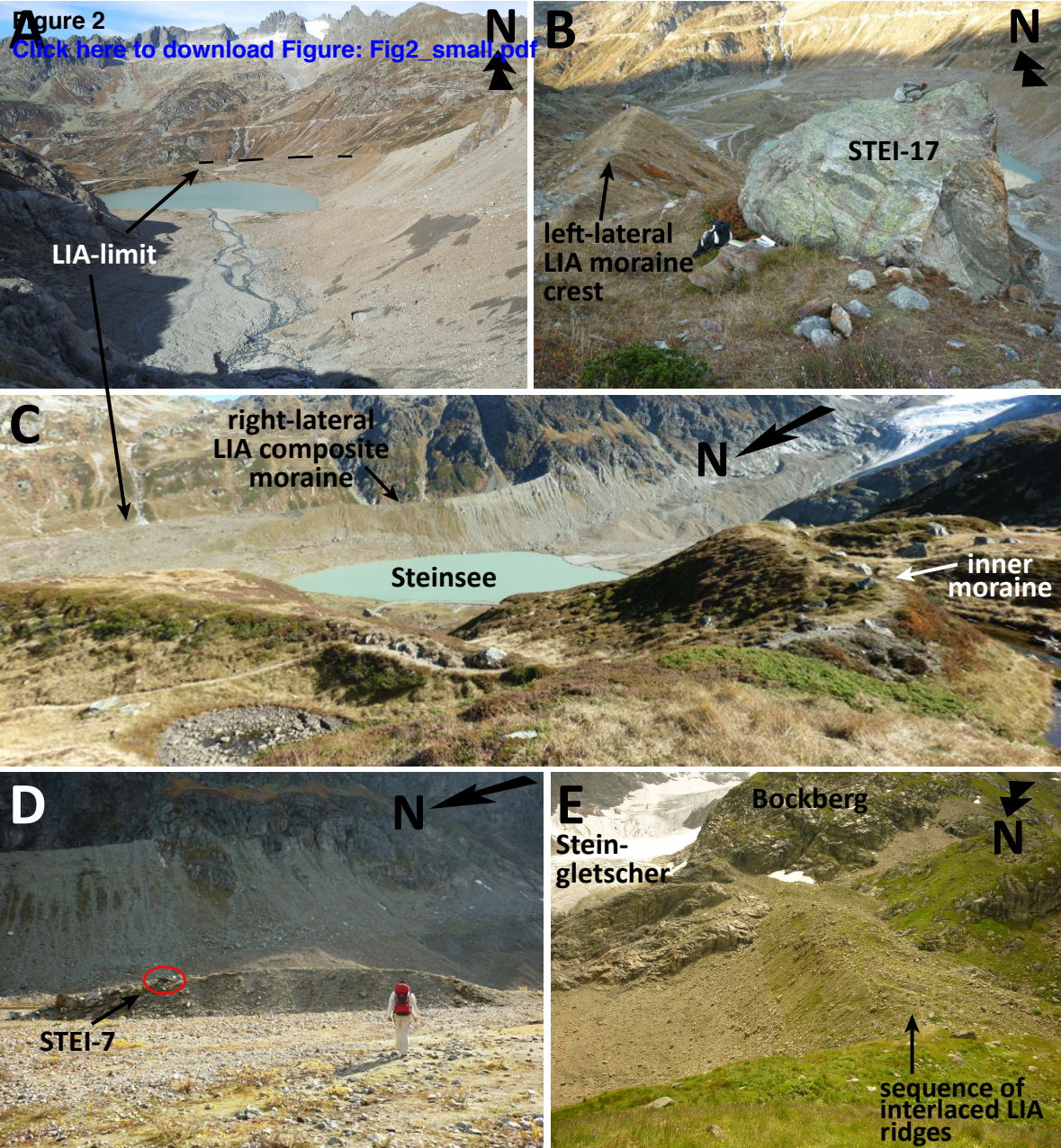


Figure 3  
[Click here to download Figure: Fig3.pdf](#)

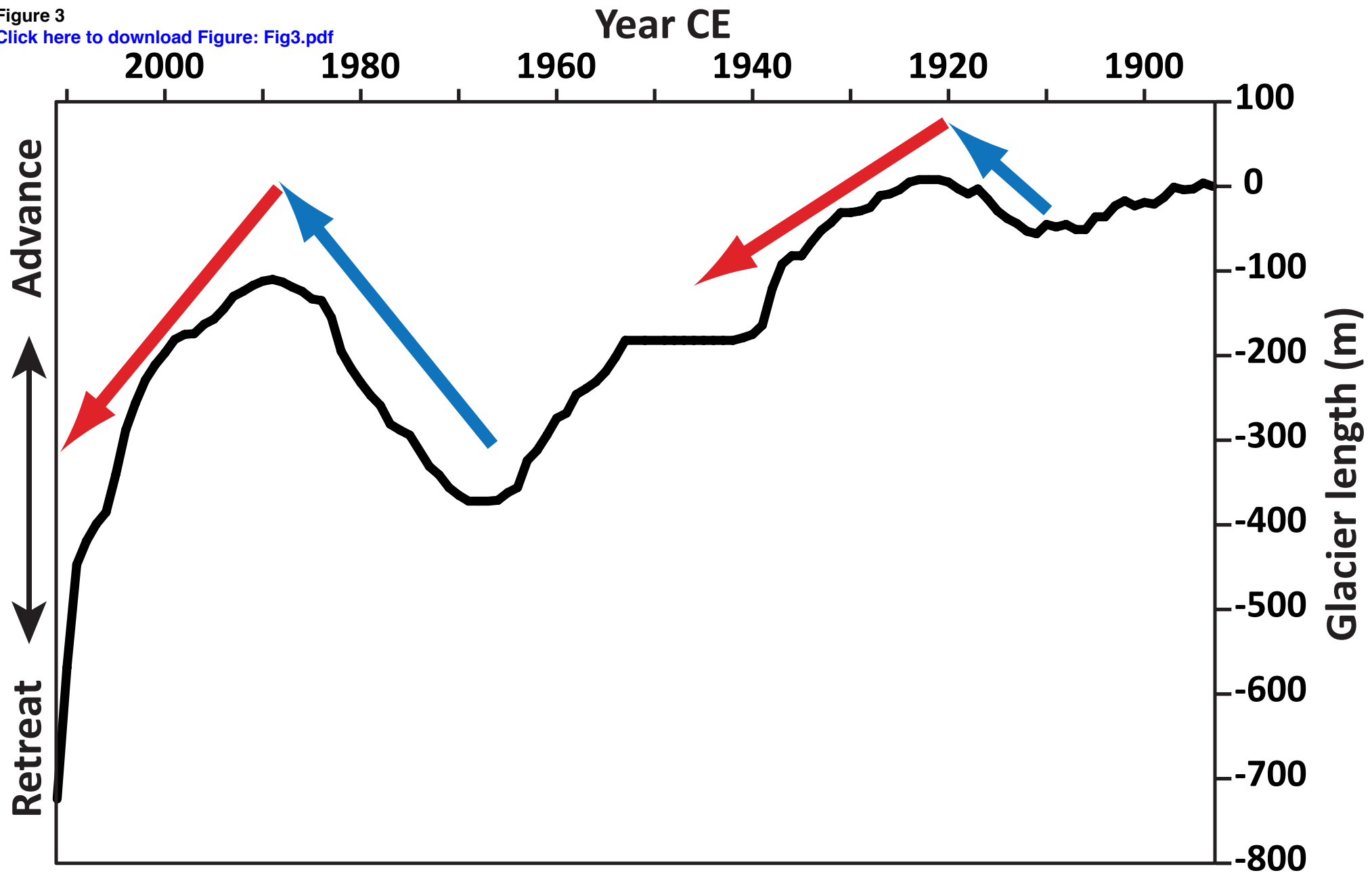


Figure 4  
[Click here to download Figure: Fig4.pdf](#)

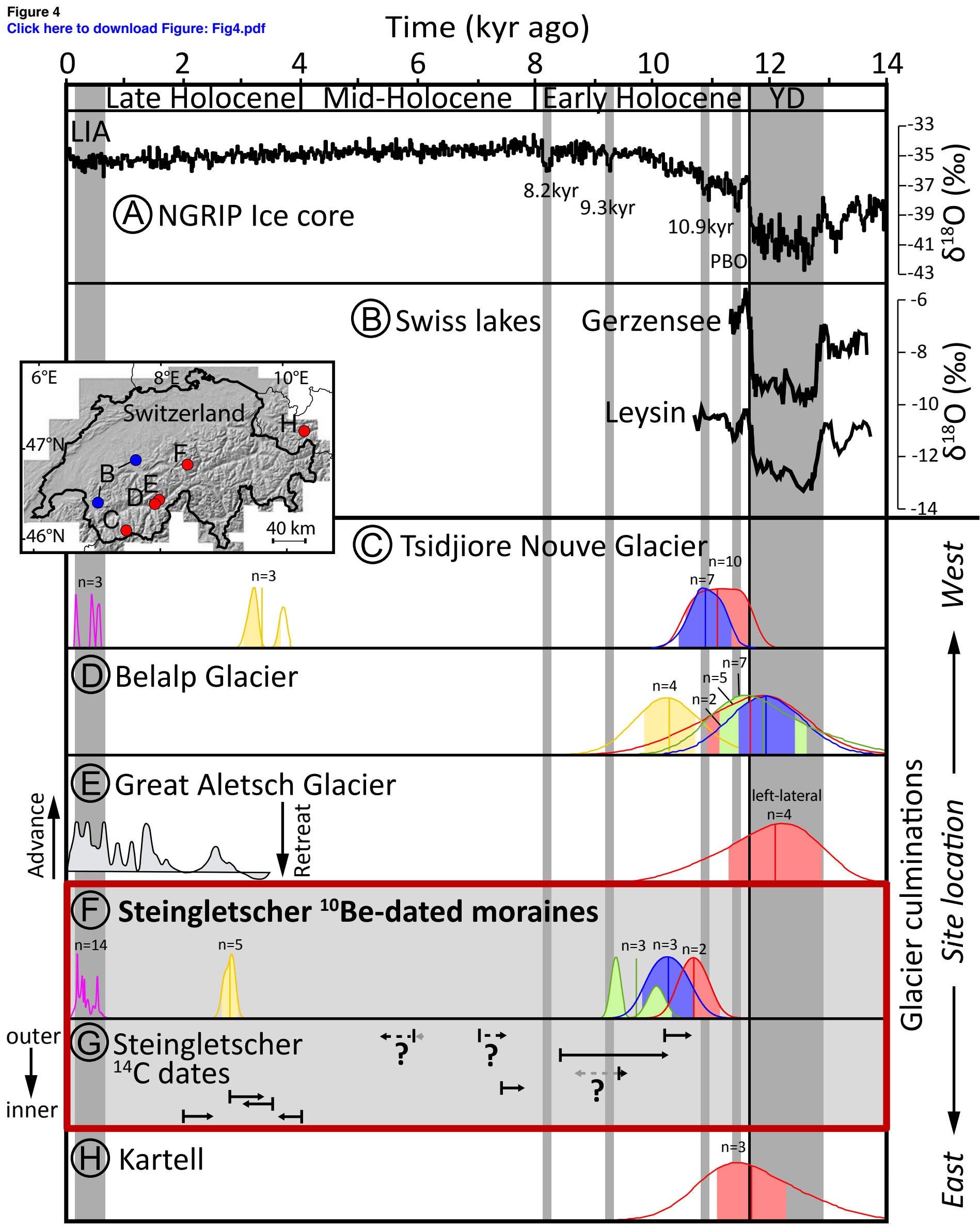
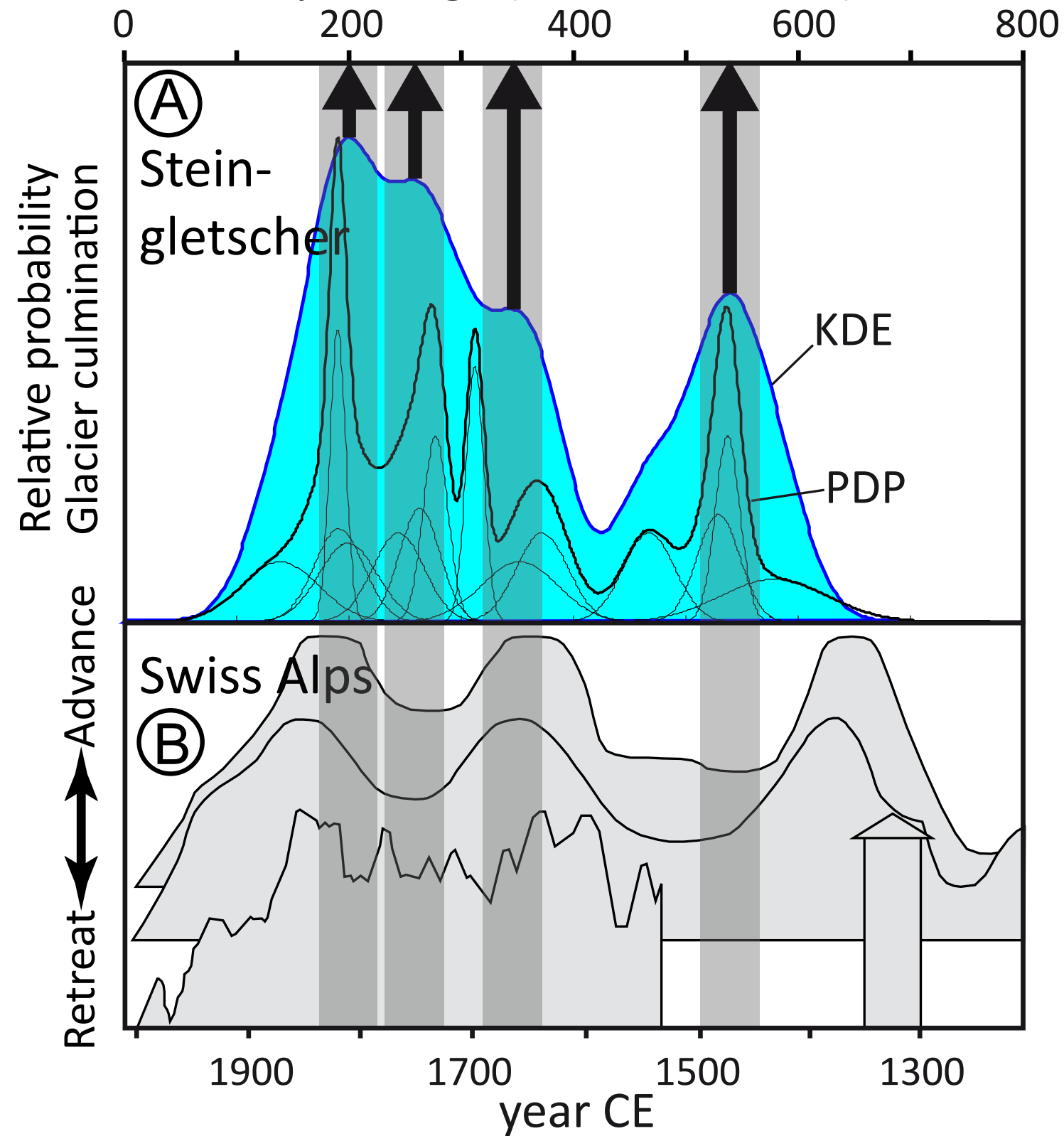


Figure 5  
[Click here to download Figure: Figs.pdf](#)



**Supplementary material for on-line publication only**

[Click here to download Supplementary material for on-line publication only: Supplement.pdf](#)